J. Fluid Mech. (1984), *vol.* 141, *pp.* 27–50
Printed in Great Britain

Stirring and transport of tracer fields by geostrophic turbulence

By GREG HOLLOWAY

Institute of Ocean Sciences, Sidney, B.C. V8L 4B2, Canada,
and School of Oceanography, University of Washington, Seattle, Washington 98195, U.S.A.

AND STEFAN S. KRISTMANNSSON

School of Oceanography, University of Washington, Seattle, Washington 98195, U.S.A.

(Received 2 December 1982 and in revised form 18 November 1983)

We investigate the interaction of concentration fields of passive tracer with velocity fields characterizing geostrophic turbulence. We develop and compare results from equilibrium statistical mechanics, from turbulence-closure theory and from numerical simulation. A consistent account emerges. Among the results we show (1) that velocity fields efficiently scatter tracer variance to all scales, (2) that tracer variance evolves toward an equilibrium spectrum which is different from the equilibrium spectrum for vorticity variance, and (3) that intermittency of the tracer field is characteristic of a cascade of tracer variance across wavenumber space. The greater efficiency of the cascade of tracer variance relative to a vorticity cascade is due to wavenumber–local advective terms which affect tracer but not vorticity. We suggest that the more efficient tracer cascade results in shorter Lagrangian autocorrelation times for tracer than for vorticity.

We investigate the spatial flux of tracer when a uniform gradient of average tracer concentration is imposed. We show (1) that the spatial flux has dominant contributions from fluctuations on scales slightly larger than the dominant energetic scales, (2) that an effective eddy-diffusivity formulation is valid and that the diffusivity agrees with simple mixing-length estimates, and (3) that eddy diffusivity is significantly anisotropic if Rossby-wave propagation occurs. Meridional diffusivity is suppressed relative to zonal diffusivity.

We complement the study of stirring down from a uniform gradient with a numerical investigation of the stirring out of an initially concentrated spot. We see that eddy diffusivity can be a dangerous concept for such problems.

1. Introduction

Large-scale distributions of water properties result from some combination of mean advection plus vertical and horizontal stirring. However, none of these fields are known in the ocean. Deep circulation is uncertain even as to the sense of the mean motion, while processes of vertical and horizontal stirring are poorly understood. Finite numbers of observations serve as constraints on possible circulation and mixing fields. In part, the vigorous eddy field, which is presumed to support horizontal stirring, frustrates efforts to observe the mean circulation either by direct observation or by inverse calculation. On the other hand, one may assume some theoretical model for circulation and then adjust coefficients of 'eddy diffusivity' to attempt to reproduce the broad features of various property distributions. Yet, even with such strong and implausible constraints as constant diffusivities, results are not unique.

Although much interest focuses on the maintenance of mean distributions, it is important to understand the statistics of fluctuations about the means. This is both a practical concern in relation to fisheries or pollution management or in relation to geochemical mapping programs and a theoretical concern in itself and in relation to the maintenance of mean distributions.

We seek more than a consistent account of observed distributions. We seek *predictive* capability in order to anticipate, for example, the effectiveness of uptake of excess CO_2 by stirring down along isopycnal surfaces or the consequences of deliberate or inadvertent release of radioactive or toxic waste substance. This means that we require a statistical-dynamical understanding of the stirring processes which result in a field of geostrophic turbulence.

There may be a further point of interest insofar as the dynamics of geostrophic turbulence are sometimes compared with models of turbulence in strongly magnetized plasmas (Hasegawa, Maclennan & Kodama 1979; Waltz 1983). The present study may bear upon problems of anomalous transport of heat (hot electrons) or doped impurity ions. In particular, as we will show how Rossby-wave propagation suppresses meridional fluxes, likewise we expect drift-wave propagation to suppress radial fluxes in a magnetically confined plasma.

2. Model equations

The variety of possible stirring environments in the ocean is diverse. In this paper we consider an idealization which may capture some of the features of large-scale oceanic stirring and transport. Suppose a vorticity field $\zeta(\boldsymbol{x}, t) = \hat{\boldsymbol{z}} \cdot \boldsymbol{\nabla} \times \boldsymbol{u}$ coevolving with a passive tracer field $\phi(\boldsymbol{x}, t)$ according to

$$\partial_t \zeta + \beta v + \boldsymbol{u} \cdot \boldsymbol{\nabla} \zeta = f + \mathrm{D}_\zeta \zeta, \tag{1a}$$

$$\partial_t \phi + \boldsymbol{u} \cdot \bar{\boldsymbol{G}} + \boldsymbol{u} \cdot \boldsymbol{\nabla} \phi = \mathrm{D}_\phi \phi. \tag{1b}$$

Here $\boldsymbol{u} = (u, v)$ is the quasi-non-divergent horizontal velocity field, β is the gradient of Coriolis parameter, $f(\boldsymbol{x}, t)$ is any field of external torques (Ekman pumping) and D_ζ is a linear operator on ζ which acts to dissipate fluctuation variance at small scales. The vorticity equation (1*a*) can be said to describe barotropic β-plane turbulence. There exists a reasonably well developed statistical-dynamical understanding for this problem (Rhines 1975, 1977; Holloway & Hendershott 1977; Basdevant *et al.* 1981). With $\beta = 0$, (1*a*) describes two-dimensional turbulence, a problem that has been widely investigated. Thus we posit (1*a*) in order to deal with a reasonably well understood vorticity or velocity field.

Equation (1*b*) gives the evolution of fluctuations ϕ about a mean tracer concentration field $\bar{\phi} = \bar{\phi}_0 + \bar{\boldsymbol{G}} \cdot \boldsymbol{x}$. D_ϕ is a linear operator on ϕ which acts to dissipate fluctuation variance at small scales. Except for effects of D_ϕ, the total tracer $\bar{\phi} + \phi$ is a conserved passive scalar field. Only $\boldsymbol{u} \cdot \bar{\boldsymbol{G}}$ acts as a source for ϕ.

Model equations (1*a*, *b*) may seem more geophysically relevant if we suppose that they represent a vertical integration between two nearby isopycnal surfaces, so that $\boldsymbol{u}$ is a parapycnal ('along-isopycnal') transport and ϕ is the vertically integrated tracer substance per unit isopycnal area. For the present level of idealization, such differences of viewpoint are only matters of taste.

We next suppose that two-point correlations of the fluctuation field vanish for large spatial separation. We then impose a constraint that fluctuations satisfy periodic boundary conditions over some large x- and y-periodicity length. This computational artifice assures that we can make an exact Fourier representation of ζ and ϕ. Physically we have in mind a large area of 'open ocean', away from lateral

boundaries. We examine a statistically homogeneous environment, hoping that our results may yet be of some value under circumstances which are not too strongly inhomogeneous. Given the present boundary conditions, we define spatial Fourier transforms of ζ and ϕ:

$$\zeta(\boldsymbol{x},t)=\sum_{\boldsymbol{k}}\zeta_{\boldsymbol{k}}(t)\,\mathrm{e}^{\mathrm{i}\boldsymbol{k}\cdot\boldsymbol{x}},\quad \phi(\boldsymbol{x},t)=\sum_{\boldsymbol{k}}\phi_{\boldsymbol{k}}(t)\,\mathrm{e}^{\mathrm{i}\boldsymbol{k}\cdot\boldsymbol{x}}. \tag{2}$$

Equations of motion for the Fourier coefficients $\zeta_{\boldsymbol{k}}$ and $\phi_{\boldsymbol{k}}$ then form an infinite set of coupled ordinary differential equations. From (1)

$$(\partial_t+\mathrm{i}\omega_{\boldsymbol{k}}+\nu_{\boldsymbol{k}})\,\zeta_{\boldsymbol{k}}=\tfrac{1}{2}\sum_{\boldsymbol{p}+\boldsymbol{q}=\boldsymbol{k}}(A_{\boldsymbol{k}\boldsymbol{p}}+A_{\boldsymbol{k}\boldsymbol{q}})\,\zeta_{\boldsymbol{p}}\,\zeta_{\boldsymbol{q}}+f_{\boldsymbol{k}}, \tag{3a}$$

$$(\partial_t+\kappa_{\boldsymbol{k}})\,\phi_{\boldsymbol{k}}=\tfrac{1}{2}\sum_{\boldsymbol{p}+\boldsymbol{q}=\boldsymbol{k}}(A_{\boldsymbol{k}\boldsymbol{p}}\,\zeta_{\boldsymbol{p}}\,\phi_{\boldsymbol{q}}+A_{\boldsymbol{k}\boldsymbol{q}}\,\zeta_{\boldsymbol{q}}\,\phi_{\boldsymbol{p}})+\mathrm{i}G_{\boldsymbol{k}}\,\zeta_{\boldsymbol{k}}, \tag{3b}$$

where $\omega_{\boldsymbol{k}}=-\beta k_x/k^2$, $A_{\boldsymbol{k}\boldsymbol{p}}=\hat{\boldsymbol{z}}\cdot(\boldsymbol{k}\times\boldsymbol{p})/p^2$ and $G_{\boldsymbol{k}}=\hat{\boldsymbol{z}}\cdot(\boldsymbol{G}\times\boldsymbol{k})/k^2$.

Fourier transforms of the operators D_ζ and D_ϕ are given by $\nu_{\boldsymbol{k}}$ and $\kappa_{\boldsymbol{k}}$. We assume that $\nu_{\boldsymbol{k}}$ and $\kappa_{\boldsymbol{k}}$ are algebraic functions of $k=|\boldsymbol{k}|$ which we are free to assign. A familiar choice, for example, is to assign $\nu_{\boldsymbol{k}}$ and $\kappa_{\boldsymbol{k}}$ after molecular viscosity and diffusion, i.e. $\nu_{\boldsymbol{k}}=\nu_0 k^2$, $\kappa_{\boldsymbol{k}}=\kappa_0 k^2$, with ν_0 and κ_0 constants. We emphasize, however, that such a choice is unfounded for the present problem. Lastly, $f_{\boldsymbol{k}}(t)$ is the transform of the external torques field $f(\boldsymbol{x},t)$.

Formally, (3*a*, *b*) are written for a countably infinite set of $\boldsymbol{k}$. We truncate that set to a large number (say 10^3 to 10^5 or so) of wavevectors by imposing a constraint that there be no interaction with any $\boldsymbol{k}$ such that $k>k_{\mathrm{T}}$, where k_{T} is some assigned truncation wavenumber. High-wavenumber truncation is justifiable if $\nu_{\boldsymbol{k}}$ and $\kappa_{\boldsymbol{k}}$ would be such as to cause only negligible fluctuation variance to occur over $k>k_{\mathrm{T}}$.

3. Statistical-equilibrium tendencies

Application of methods of equilibrium statistical mechanics to large-scale geophysical flows has been developed in Salmon, Holloway & Hendershott (1976) and Frederiksen & Sawford (1980). We focus attention on the role of nonlinear terms, viz $\zeta\zeta$ and $\zeta\phi$ in (3). Such terms are often poorly understood, usually requiring perturbation treatments of dubious validity. Here we adopt quite a different approach, omitting all forcing and dissipation terms, i.e. taking $\nu_{\boldsymbol{k}}=\kappa_{\boldsymbol{k}}=f_{\boldsymbol{k}}=G_{\boldsymbol{k}}=0$ in (3). Then the conjecture is that, after some unspecified time, solutions of (3) from almost any initial condition will tend toward a state of 'maximal randomness' or maximum entropy (to be defined below). The only constraints on the maximum entropy solution are that quantities which are conserved globally under nonlinear interactions will retain their initial values (on average) in the maximum entropy solution.

For the truncated, unforced (both f and $\overline{\boldsymbol{G}}$ vanish), nondissipative set of equations (3), there are four conserved quantities:

$$\text{energy}\quad \bar{E}=\tfrac{1}{2}\sum_{\boldsymbol{k}}|\zeta_{\boldsymbol{k}}|^2/k^2, \tag{4a}$$

$$\text{vorticity variance}\quad \bar{Z}=\sum_{\boldsymbol{k}}|\zeta_{\boldsymbol{k}}|^2, \tag{4b}$$

$$\text{tracer variance}\quad \bar{Q}=\sum_{\boldsymbol{k}}|\phi_{\boldsymbol{k}}|^2, \tag{4c}$$

$$\zeta\text{-}\phi\text{ correlation}\quad \bar{C}=\Sigma\,\mathrm{Re}\,\langle\zeta_{\boldsymbol{k}}\,\phi_{\boldsymbol{k}}^*\rangle. \tag{4d}$$

A general specification of entropy which is consistent both with classical statistical mechanics and with information theory (Shannon 1948) is given in terms of probability distributions of solutions. Imagine a phase space in which coordinates y_i consist of the real and imaginary parts of the various ζ_k and ϕ_k. Let $P(\{y\}, t)$ be a probability distribution determined from some initial distribution and evolving following solutions to (3). Entropy is

$$S(t) = -\int P(\{y\}, t) \ln P(\{y\}, t) \Pi \, \mathrm{d}y_i. \tag{5}$$

For a wide range of problems, including the present problem, conserved quantities can be cast in quadratic forms, hence written as constraints on the second-order correlation matrix

$$Y_{ij} = \langle y_i y_i \rangle, \tag{6}$$

where $\langle\ \rangle$ indicates an average over P. Carnevale, Frisch & Salmon (1981) show that the extremal S for given Y_{ij} is

$$S(t) = \tfrac{1}{2} \ln \det Y_{ij}(t) \tag{7}$$

plus a constant which depends on the dimension of phase space. We seek Y_{ij} that maximizes S subject to (4). In terms of mode variances $Z_k = \langle |\zeta_k|^2 \rangle$ and $Q_k = \langle |\phi_k|^2 \rangle$, the results are simple equipartition forms

$$Z_k = \frac{k^2}{\alpha_1 + \alpha_2 k^2}, \tag{8a}$$

$$Q_k = \alpha_3^{-1} \tag{8b}$$

(cf. Kraichnan 1967), and we suppose $\bar{C} = 0$ for the present discussion. Constants α_i are evaluated from the condition that (8) satisfy (4). Note that these results are independent of the value of β. Numerical simulations showing vorticity evolution toward (8a) have been described by Deem & Zabusky (1971), Fox & Orszag (1973) and Bennett & Haidvogel (1983). Below we will describe a simulation showing simultaneous vorticity and tracer evolution toward (8a, b).

It is important to emphasize – strongly – that (8a, b) are not themselves physically plausible results. The neglect of dissipation together with finite truncation of (3) is not physically admissible. Nonetheless, arguments leading to (8) are quite useful for the three following reasons.

(a) Although the role of dissipation will prevent physical solutions of (3) from approaching (8), still the statistical tendencies due to nonlinear terms are to drive solutions *toward* (8). More precisely, nonlinear terms will cause positive growth, on average, of entropy (7), even though dissipation may result in net loss of entropy from the macroscopic fluctuation fields. This tendency toward increasing entropy can be demonstrated explicitly for turbulence-closure theories of the type described in §4 (cf. Carnevale *et al.* 1981).

(b) We will be able to identify terms arising in turbulence-closure theory which explicitly drive solutions toward (8). This will aid us in organizing the formidable algebra that is generated from closure theory.

(c) Intermittency, which we here quantify by the occurrence of non-Gaussian moments of $P(\{y\})$, vanishes at the maximum-entropy solution (8). Thus we associate intermittency with processes that drive solutions *toward* (8), i.e. with the transfer of variances across $\boldsymbol{k}$-space.

The point of this section is to note the relatively simple solutions, viz (8), at one

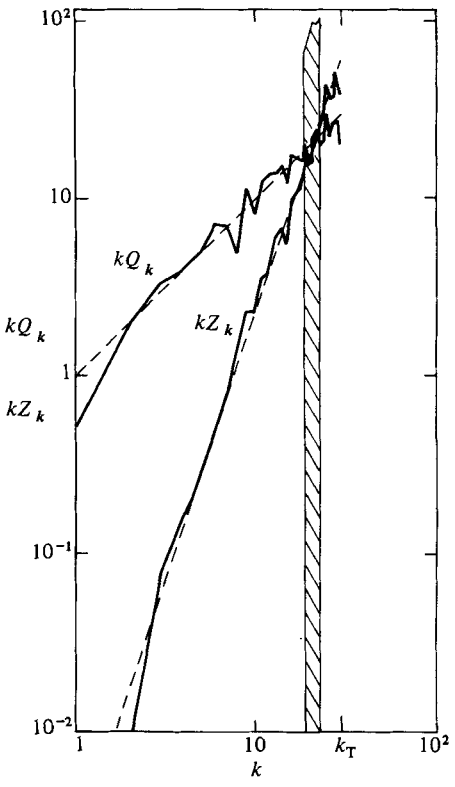

FIGURE 1. Spectra of tracer variance and of vorticity variance illustrate the evolution of unforced, non-dissipative flow. One-dimensional spectra shown in the figure are the sums of modal variances Q_k and Z_k in circular wavebands of radius $k = |\boldsymbol{k}|$. Initial spectra of tracer (Q_k) and of vorticity (Z_k) are identical, shown shaded. At later time Q_k and Z_k, shown as solid curves, have approached their separate equipartition or maximum entropy solutions, shown as dashed curves. Truncation is at $k_T = 30$.

limit of the parameter space of (3). We may also observe some subtle character of the statistical dynamics. Consider the following apparent paradox.

Let an initial field consist of a random phase assignment of a vorticity field according to a prescribed variance spectrum Z_k. Independently (i.e. $\bar{C} = 0$) initialize a random-phase tracer field with spectrum Q_k identical with Z_k. Let the fields evolve according to (3) in the case of $\nu_k = \kappa_k = f_k = G_k = \beta = 0$. On one hand we might suppose that, since the initial fields are statistically identical, and since each field evolves only owing to advection by the same velocity field, the subsequent evolution of Z_k and Q_k will be identical. On the other hand, depending upon the initial (and conserved) values of $\bar{E}$, $\bar{Z}$ and $\bar{Q}$, equipartition results (8) show that Z_k and Q_k may evolve quite differently. Which occurs? In figure 1 a direct numerical simulation (64×64 resolution, pseudospectral, dealiased) clearly shows the dissimilar evolution of Z_k and Q_k toward their respective forms (8*a*, *b*). The two initial conditions are not statistically identical insofar as vorticity is directly related to the velocity field.

4. Turbulence-closure theory

Methods of equilibrium statistical mechanics, as seen in § 3, are relatively easy to apply and may be insightful from the view of certain mathematical limits of (3). However, actual fluid systems do not approach absolute equilibrium (8) closely on account of the essential role of dissipation. Actual fluids must be viewed as 'open' systems in thermodynamic contact with the field of molecular agitation (including in the present cases the field of unresolved smaller-scale motions). Flows may approach a condition of statistical stationarity, but such a condition will be the result of competing disequilibrium processes including forcing, dissipation and variance transfer.

Quantitative theoretical treatment for disequilibrium statistical fluid mechanics is not well developed. We borrow upon turbulence theory, in particular the class of 'eddy-damped quasi-normal Markovian' (EDQNM) closures. Discussions of EDQNM may be found in Leslie (1973), Orszag (1977) and Rose & Sulem (1978). The purpose is to obtain a closed set of equations describing the wavenumber distribution of single-time variances in a state close to statistical stationarity. Our approach is given altogether in terms of Eulerian field statistics. This approach is an alternative to a more classical line of development in which concentration-fluctuation statistics and transport rates are inferred from stochastic models of Lagrangian particle trajectories (Taylor 1921; Thiebaux 1975; Chatwin & Sullivan 1980; Durbin 1980; Davis 1983).

Application of EDQNM is relatively straightforward but algebraically tedious. Closure for β-plane turbulence (3a) has been developed and discussed in Holloway & Hendershott (1977). Closure for (3b) with $G_k = 0$ has been given in Holloway (1976) and discussed by Lesieur, Sommeria & Holloway (1981). With $G_k \neq 0$, the problem becomes more complicated, but very much more interesting.

We begin by writing ensemble-averaged second-moment equations. Multiplying (3a, b) each by ζ_k^* and ϕ_k^*, where $*$ denoted complex conjugate, and then adding conjugate equations, we have

$$(\partial_t + 2\nu_k) Z_k = \sum_{p+q=k} (A_{kp} + A_{kq}) \operatorname{Re} \langle \zeta_k^* \zeta_p \zeta_q \rangle + F_k, \tag{9a}$$

$$(\partial_t + 2\kappa_k) Q_k = \sum_{p+q=k} (A_{kp} \operatorname{Re} \langle \phi_k^* \zeta_p \phi_q \rangle + A_{kq} \operatorname{Re} \langle \phi_k^* \zeta_q \phi_p \rangle) - 2G_k \operatorname{Im} \Gamma_k, \tag{9b}$$

$$\begin{aligned}(\partial_t + \mathrm{i}\omega_k + \nu_k + \kappa_k) \Gamma_k = {} & \tfrac{1}{2} \sum_{p+q=k} (A_{kp} \langle \zeta_k \zeta_p^* \phi_q^* \rangle \\ & + A_{kq} \langle \zeta_k \zeta_q^* \phi_p^* \rangle + (A_{kp} + A_{kq}) \langle \phi_k^* \zeta_p \zeta_q \rangle) - \mathrm{i} G_k Z_k + \langle f_k \phi_k^* \rangle,\end{aligned} \tag{9c}$$

where $Z_k = \langle \zeta_k \zeta_k^* \rangle$, $Q_k = \langle \phi_k \phi_k^* \rangle$), $\Gamma_k = \langle \zeta_k \phi_k^* \rangle$) and F_k collects the effective forcing of Z_k due to any external torques.

It will be useful to note some relations. Because $\zeta(\boldsymbol{x}, t)$ and $\phi(\boldsymbol{x}, t)$ are real fields,

$$\zeta_{-k} = \zeta_k^*, \quad \phi_{-k} = \phi_k^*. \tag{10}$$

Z_k and Q_k are real, while Γ_k is complex. From (10)

$$Z_{-k} = Z_k, \quad Q_{-k} = Q_k, \quad \Gamma_{-k} = \Gamma_k^*. \tag{11}$$

The various triple-moment terms in (9) will produce variance transfer. We will address these terms below. The $G_k \Gamma_k$ terms in (9b) is a source of tracer variance due to a spatial flux of tracer down the mean gradient $\boldsymbol{G}$. That spatial flux is given by

$$\langle \boldsymbol{u} \phi \rangle = \sum_k \frac{\boldsymbol{k} \times \hat{\boldsymbol{z}}}{k^2} \operatorname{Im} \Gamma_k. \tag{12}$$

$G_k Z_k$ in (9*c*) acts as a source for $\mathrm{Im}\, \Gamma_k$, which, through (9*b*), provides a source for Q_k. A term $\langle f_k \phi_k^* \rangle$ arises from the forcing of vorticity. For present purposes we will omit $\langle f_k \phi_k^* \rangle$.

Carrying onward from (9), we would construct evolution equations for the various triple-moment terms. The number of equations and the number of terms in each equation proliferate rapidly. Yet the problem remains unclosed since each set of equations for Nth moments will involve terms in $(N+1)$th moments as well as all lower-order moments.

Closure is effected by a 'cumulant hypothesis'. For the present case, all fourth moments are reduced to a part due to products of variance and a residual part or 'fourth cumulant'. A possible hypothesis is to discard (set to zero) all fourth cumulants. Indeed most theory of weak wave–wave interaction corresponds to zero fourth cumulant. However, for stronger interactions such as in turbulence, fourth-cumulant discard is known to fail.

EDQNM makes two hypotheses: (1) that fourth cumulants act to relax triple moments, and (2) that second moments evolve on timescales longer than triple-moment relaxation times. The second hypothesis is just the condition for quasi-stationarity, and we assume that it holds. Differences among EDQNM treatments focus on different means for specifying triple-moment relaxation times. For the present we may proceed simply by assuming a single, unspecified time constant τ (cf. Frisch, Lesieur & Brissand 1974). Later we may select a more suitable relaxation time dependent upon the $(\boldsymbol{k},\boldsymbol{p},\boldsymbol{q})$-triad of interest.

Despite these simplifying assumptions, EDQNM treatment of (9) remains tedious and not very insightful. We invoke a further simplification. Either by considering flows only long after initiation or by considering only flows initiated with zero tracer fluctuations, we may retain only terms which cause Γ_k to be proportional to $|\boldsymbol{G}|$. This condition is required from dimensional consistency. It means that we have discarded a number of terms that serve to describe the decay of initial transients.

Proceeding from (9*a*) after Holloway & Hendershott (1977), we have

$$(\partial_t + 2\nu_k + 2\eta_k) Z_k = \Lambda_k + F_k, \tag{13a}$$

where

$$\eta_k = \sum_{p+q=k} \tau b_{kpq} Z_p, \tag{13b}$$

$$\Lambda_k = \sum_{p+q=k} \tau a_{kpq} Z_p Z_q \tag{13c}$$

and

$$a_{kpq} = |\boldsymbol{k} \times \boldsymbol{p}|^2 \left(\frac{1}{p^2} - \frac{1}{q^2}\right)^2, \tag{13d}$$

$$b_{kpq} = |\boldsymbol{k} \times \boldsymbol{p}|^2 \left(\frac{1}{p^2} - \frac{1}{q^2}\right)\left(\frac{1}{p^2} - \frac{1}{k^2}\right). \tag{13e}$$

Similarly, from (9*b*)

$$(\partial_t + 2\kappa_k + 2\gamma_k) Q_k = \Phi_k - 2G_k \,\mathrm{Im}\, \Gamma_k, \tag{14a}$$

where

$$\gamma_k = \sum_{p+q=k} \tau c_{kpq} Z_p, \tag{14b}$$

$$\Phi_k = 2 \sum_{p+q=k} \tau c_{kpq} Z_p Q_q \tag{14c}$$

and

$$c_{kpq} = \frac{|\boldsymbol{k} \times \boldsymbol{p}|^2}{p^4}. \tag{14d}$$

Finally, from (9*c*)

$$(\partial_t + \mathrm{i}\omega_k + \nu_k + \eta_k + \gamma_k)\,\Gamma_k = -\mathrm{i}G_k Z_k, \tag{15}$$

where η_k and γ_k are given in (13*b*) and (14*b*). A large number of terms involving sums over products GZZ, ΓZ, ΓQ or $\Gamma\Gamma$ have been discarded in (14) and (15) either because they fail to yield Γ proportional to $|G|$ or correspondingly Q proportional to $|G|^2$. Other terms arising in the Γ-equation due to non-stationarity of Z have been discarded. An exception to these rules occurs in (14*a*). We do not discard Φ_k, because we cannot argue that initial tracer varianee will decay except through explicit dissipation κ_k. We retain terms that are sufficient to account for known or plausible physics, rejecting terms that play incidental roles related to non-stationary problems. Expressions similar to (14) and (15) are discussed also in Hill (1981).

As a last note in this section, we recall the unforced non-dissipative case $\nu_k = \kappa_k = f_k = G_k = 0$. It may be verified by substitution that (8) together with $\Gamma_k = 0$ are stationary solutions to (13)–(15). By the H-theorem (Carnevale *et al.* 1981) these are the only stable solutions.

5. Timescales for variance transfers

When comparing vorticity and passive-tracer evolution, one of the important features is that a passive tracer (uncorrelated with vorticity) exhibits more rapid spectral evolution than vorticity. This feature is easily identified in the closure equations (13) and (14). Supposing negligible ν_k and κ_k over most k, the timescale for vorticity variance is given by η_k while the timescale for tracer variance is given by γ_k. We compare the two rates:

$$\begin{aligned}\gamma_k - \eta_k &= \tfrac{1}{2}\Sigma\tau(c_{kpq}Z_p + c_{kpq}Z_q - b_{kpq}Z_p - b_{kpq}Z_q)\\ &= \tfrac{1}{2}\Sigma\tau\frac{|\boldsymbol{k}\times\boldsymbol{p}|^2}{k^2p^2q^2}\{k^2(Z_p+Z_q)+(p^2-q^2)(Z_q-Z_p)\}.\end{aligned} \tag{16}$$

The first term in curly brackets is positive. The second term is positive for that portion of the spectrum on which Z_k is a decreasing function of increasing $|\boldsymbol{k}|$, which is usually the domain of interest. Hence there is a strong preference for $\gamma_k > \eta_k$, i.e. shorter timescales for tracer-variance evolution.

Differences between the evolution of tracer and vorticity variances are due to the roles of local interaction terms. In many turbulent phenomena, local interactions $k \approx p \approx q$ are most effective. Such interactions are effective in the tracer equation (14). However, the vorticity equation in two dimensions excludes just these local interactions. If any two of three wavenumbers are nearly equal then b_{kpq} tends to vanish.

We can easily see this tendency in physical space by considering a very narrow band spectrum peaked near some k_0. Then $\zeta \approx -k_0^2\Psi$ and flow is nearly along isolines of vorticity. Advective terms tend to vanish as

$$\boldsymbol{u}\cdot\nabla\zeta = \mathrm{J}(\Psi,\zeta) \approx -k_0^2\,\mathrm{J}(\Psi,\Psi) = 0, \tag{17}$$

where J denotes the Jacobian determinant with respect to x, y. Narrow-bandedness imposes no such constraint on the advection $\boldsymbol{u}\cdot\nabla\phi$ of tracer.

Numerical simulations show the dramatically different appearance of $\phi(\boldsymbol{x},t)$ and $\zeta(\boldsymbol{x},t)$. In figure 2 from 128×128 resolution experiment, ϕ and ζ are initially uncorrelated fields with identical spectra. $F_k = G_k = \beta = 0$, while small-scale diffusion of molecular type, i.e. $\nu_k = \nu_0 k^2$ and $\kappa_k = \kappa_0 k^2$, have identical coefficients $\nu_0 = \kappa_0$.

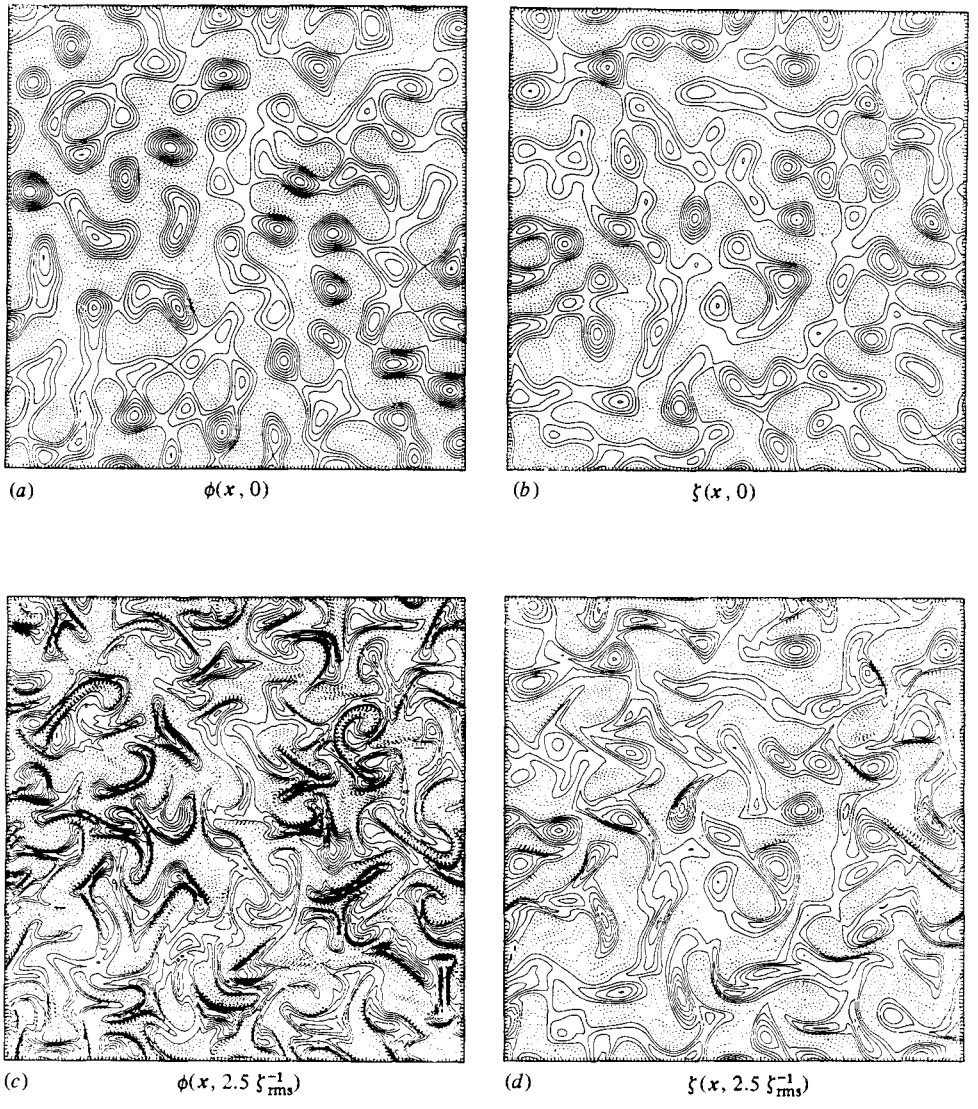

FIGURE 2. Differences in the physical appearances of ϕ- and of ζ-fields are seen. (*a*) and (*b*) show initial fields of ϕ and of ζ. The fields are uncorrelated but have identical variance spectra. (*c*) and (*d*) show ϕ and ζ respectively, at later time $t = 2.5\zeta_{\mathrm{rms}}^{-1}$. Identical coefficients of diffusion $\nu_0 = \kappa_0$ act on the fields. $\overline{G} = f = \beta = 0$. Enhanced scattering of ϕ to small scales is readily seen.

It is seen that ϕ rapidly scatters to small scales. An immediate consequence of possible geophysical relevance is that variance of passive tracer is dissipated more rapidly than vorticity variance. Although the more rapid transfer of tracer variance has been deduced (and verified numerically) as a result for Eulerian fields, we may also make an inference regarding Lagrangian particles. When $F_k = G_k = \beta = 0$, then a Lagrangian particle will conserve the vorticity ζ and tracer ϕ except through direct effects of non-conservative operators D_ζ and D_ϕ in (1). When Lagrangian particles are tracked in an Eulerian-based simulation, further non-conservative terms arise owing to both finite interpolation and to aliasing terms which are cancelled in the Eulerian simulation but which do not cancel along Lagrangian trajectories (Haidvogel

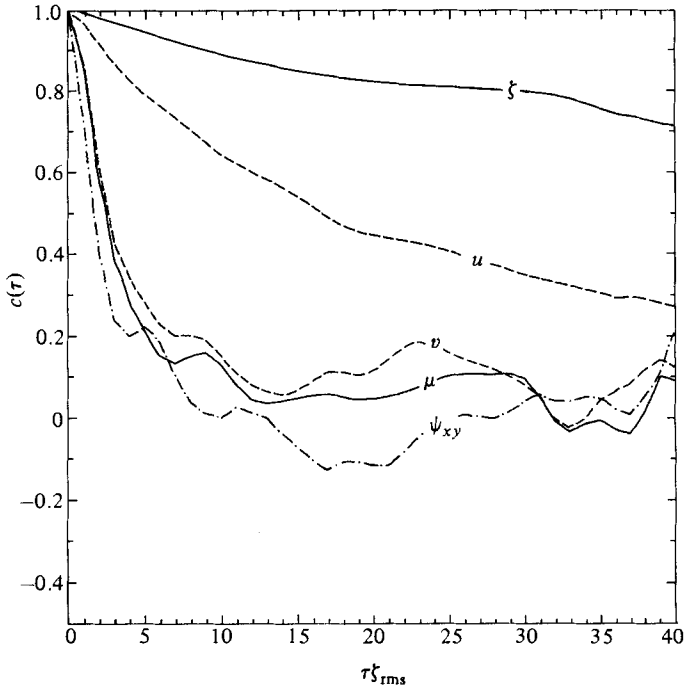

FIGURE 3. Lagrangian autocorrelation functions $C_q(\tau)$ for various fields: $q = u$, $q = v$, $q = \zeta$, $q = \partial^2\psi/\partial x\,\partial y$ and $q = \phi$.

1982). However, to the extent that an inertial cascade of vorticity and tracer variance dominates particle dynamics, it is plausible that particle 'memory' of initial tracer ϕ is erased more quickly than 'memory' of initial vorticity ζ. To test this conjecture, particles were tracked in a simulation similar to that seen in figure 2. Normalized Lagrangian autocorrelations $C_q(\tau)$ were calculated for various fields: $q = u$, $q = v$, $q = \zeta$, $q = \partial^2\psi/\partial x\,\partial y$ and $q = \phi$. Results, averaged over 48 particles, are seen in figure 3. Strongly non-conserved quantities such as u, v or $\partial^2\psi/\partial x\,\partial y$ are effectively decorrelated after about $\pi\zeta_{\mathrm{rms}}^{-1}$. Quantities ζ and ϕ, which would be conserved except for explicit dissipation operators and alias errors, decorrelate less rapidly. It is clear though that ϕ decorrelates more quickly than ζ does.

6. Eddy-diffusivity tensor

While fluctuation spectra are interesting in themselves and important, e.g. to the design of a mapping program, the single item of most common practical concern is an 'eddy diffusivity' defined by

$$\langle \boldsymbol{u}\phi \rangle = -\boldsymbol{D}\cdot\boldsymbol{G}, \tag{18}$$

where $\boldsymbol{D}$ is the eddy-diffusivity tensor in the horizontal (or parapycnal) surface. Commonly $\boldsymbol{D}$ is assumed to be isotropic (in the horizontal or parapycnal surface). Then the right-hand side of (18) is simply $-A_{\mathrm{H}}\boldsymbol{G}$, with A_{H} an *ad hoc* 'coefficient of eddy diffusivity', which might be assigned or fitted to observations or estimated by 'mixing length' as $l'u'$, with l' a characteristic length and u' a characteristic velocity of the eddy field. Often A_{H} is treated not only as a constant but, practically, as a thermodynamic property of seawater. Estimates based on large-scale distributions give diverse values for A_{H} (see e.g. Sverdrup, Johnson & Fleming 1942). An explicit

model illustrating effects of spatial variation and anisotropy of $\boldsymbol{D}$ is described by Armi & Haidvogel (1982). However, the nature of variation and the extent of anisotropy were specified in an *ad hoc*, though plausible, way. One purpose of the present study is to provide a more theoretical basis for such specifications.

Efforts to model fluxes in the Fickian form (18) depend upon the mean $\bar{\phi}$-concentration varying on lengthscales large compared with the largest energetic eddy lengthscales. In geophysical reality this condition may not hold anywhere, and certainly will not hold everywhere. Thus we are cautioned from assuming even the existence of a diffusivity, apart from its value.

For the present theory and numerical experiments, we have assumed a uniform mean gradient G and hence an infinite lengthscale separation from the turbulent field, which is constrained to satisfy periodic boundary conditions. Therefore we expect to find a diffusivity representation of the form (18). We do so by examining the spectral contributions to $\langle \boldsymbol{u}\phi \rangle$ according to (12). From (15) the stationary solution for $\operatorname{Im} \Gamma_{\boldsymbol{k}}$ is

$$\operatorname{Im} \Gamma_{\boldsymbol{k}} = -\frac{\xi_{\boldsymbol{k}} G_{\boldsymbol{k}} Z_{\boldsymbol{k}}}{\omega_{\boldsymbol{k}}^2 + \xi_{\boldsymbol{k}}^2}, \tag{19}$$

where $\xi_{\boldsymbol{k}} = \nu_{\boldsymbol{k}} + \kappa_{\boldsymbol{k}} + \eta_{\boldsymbol{k}} + \gamma_{\boldsymbol{k}}$ for convenience. From (12), in component notation,

$$\langle (u_1, u_2)\, \phi \rangle = \sum_{\boldsymbol{k}} (-k_2, k_1) \frac{\xi}{\xi_{\boldsymbol{k}}^2 + \omega_{\boldsymbol{k}}^2} \frac{Z_{\boldsymbol{k}}}{k^4} (G_1 k_2 - G_2 k_1), \tag{20}$$

where $\boldsymbol{u} = (u, v) = (u_1, u_2)$, $-\boldsymbol{k} \times \hat{\boldsymbol{z}} = (-k_2, k_1)$ and $\boldsymbol{G} = (G_1, G_2)$. In $\boldsymbol{k}$-space we adopt a polar representation

$$\boldsymbol{k} = k (\cos \theta_{\boldsymbol{k}}, \sin \theta_{\boldsymbol{k}}), \tag{21a}$$

$$\omega_{\boldsymbol{k}}^2 = \frac{\beta^2}{2k^2} (1 + \cos 2\theta_{\boldsymbol{k}}), \tag{21b}$$

$$Z_{\boldsymbol{k}} = \sum_{n=-\infty}^{\infty} Z_n(k)\, \mathrm{e}^{\mathrm{i}n\theta_{\boldsymbol{k}}}. \tag{21c}$$

From $Z_{-\boldsymbol{k}} = Z_{\boldsymbol{k}}$ and real $Z_{\boldsymbol{k}}$, Z_n vanish for odd n while $Z_{-n} = Z_n^*$. We truncate (21c) at $|n| = 2$. Then the coefficient of $\cos 2\theta_{\boldsymbol{k}}$ gives a tendency to prefer zonal or meridional motion, while the coefficient of $\sin 2\theta_{\boldsymbol{k}}$ would give tendency to prefer NW–SE or NE–SW motion. There is no tendency on a β-plane to excite the $\sin 2\theta_{\boldsymbol{k}}$ coefficient, so we assume that it vanishes. We rewrite (21c) in a more useful form:

$$Z_{\boldsymbol{k}} = \frac{Z(k)}{2\pi k} (1 - R(k) \cos 2\theta_{\boldsymbol{k}}), \tag{22}$$

where now $Z(k)$, i.e. without subscript, is the isotropic (power) spectrum for vorticity and $R > 0$ gives a tendency to prefer zonal over meridional flows, whereas $R < 0$ gives the reverse tendency.

Following Rhines (1975) and Holloway & Hendershott (1977), there is a known tendency on the β-plane to develop anisotropy preferring zonal motions ($R > 0$). For the present we ignore anisotropy in $\xi_{\boldsymbol{k}}$ for lack of other information and denote the isotropic part by $\xi(k)$.

Replacing wavevector sums $\Sigma_{\boldsymbol{k}}$ with sums $\Sigma_k \int_0^{2\pi} k\, \mathrm{d}\theta$, where $k = |\boldsymbol{k}|$, (20) becomes

$$\begin{aligned} \langle (u_1, u_2)\, \phi \rangle &= \sum_k \frac{\xi(k)\, Z(k)}{2\pi k^2} \int_0^{2\pi} \mathrm{d}\theta\, (-\sin\theta, \cos\theta) \frac{(1 - R\cos 2\theta)\, (G_1 \sin\theta - G_2 \cos\theta)}{\xi^2 + \dfrac{\beta^2}{2k} (1 + \cos 2\theta)} \\ &= -(G_1, G_2) \sum_k \boldsymbol{D}(k), \end{aligned} \tag{23}$$

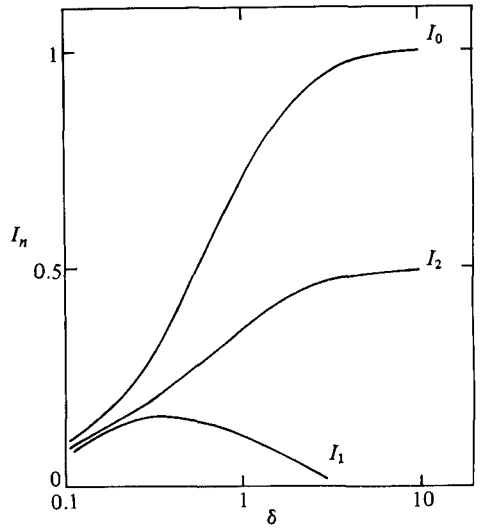

FIGURE 4. Integrals $I_n(\delta)$ as defined in (26).

where $\boldsymbol{D}(k)$ are contributions to the diffusivity tensor $\boldsymbol{D}$. Components of $\boldsymbol{D}(k)$ are

$$D_{11}(k) = \frac{Z(k)}{k^2\xi(k)}[I_0(\delta) + (R(k)+1)\,I_1(\delta) + R(k)\,I_2(\delta)], \tag{24a}$$

$$D_{22}(k) = \frac{Z(k)}{k^2\xi(k)}[I_0(\delta) + (R(k)-1)\,I_1(\delta) - R(k)\,I_2(\delta)], \tag{24b}$$

$$D_{12} = D_{21} = 0, \tag{24c}$$

where

$$\delta(k) = k\xi(k)/\beta \tag{25}$$

is a measure of the tendency for turbulence relative to wave propagation. Integrals in $I_n(\delta)$ are of the form

$$I_n(\delta) = \frac{(-1)^n}{2\pi}\int_0^{2\pi} \frac{\cos^n\theta}{1+\dfrac{1+\cos\theta}{2\delta^2}}\,\mathrm{d}\theta, \tag{26a}$$

yielding

$$I_0 = \frac{\delta}{(\delta^2+1)^{\frac{1}{2}}}, \tag{26b}$$

$$I_1 = \frac{2\delta^3+\delta}{(\delta^2+1)^{\frac{1}{2}}} - 2\delta^2, \tag{26c}$$

$$I_2 = \frac{4\delta^5+4\delta^3+\delta}{(\delta^2+1)^{\frac{1}{2}}} - 4\delta^4 - 2\delta^2. \tag{26d}$$

Graphs of $I_n(\delta)$ are shown in figure 4.

The result (24) can be readily interpreted. Coefficients $Z/k^2\xi$ show that contributions to diffusivity from scales k vary as the local velocity variance Z/k^2 multiplied by a time ξ^{-1} which is a kind of persistence time for turbulent motions of scale k. For the special case of isotropic turbulence without β, $I_1 = R = 0$ while $I_0 = 1$ and $I_2 = \frac{1}{2}$. Then $\boldsymbol{D}$ is isotropic and given by a single coefficient:

$$A_{\mathrm{H}} = \sum_k \frac{Z_k}{k^2\xi_k}. \tag{27}$$

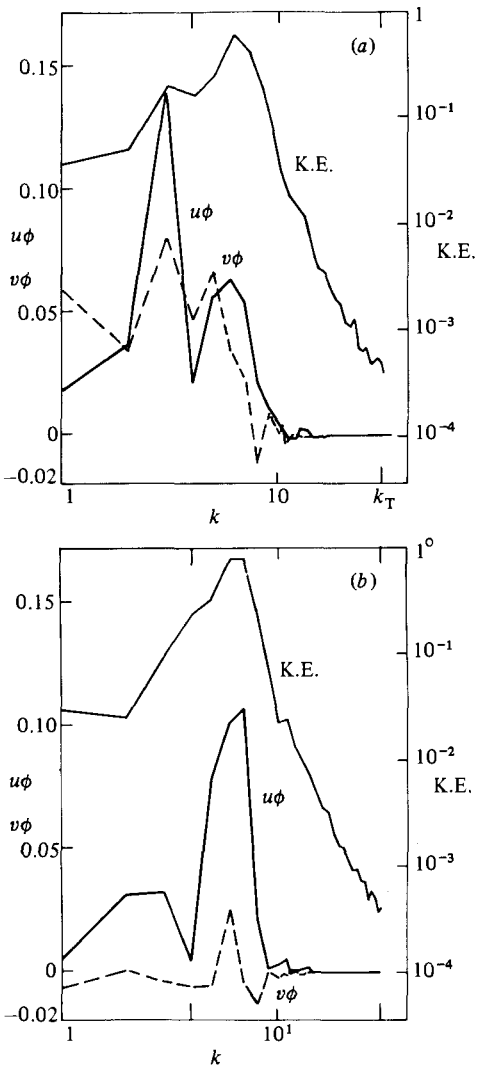

FIGURE 5. Spectral decomposition of the zonal flow $u\phi$ is shown solid while meridional flux $v\phi$ is shown dashed. Kinetic energy spectra are shown: (*a*) $\beta = 0$; (*b*) $\beta \neq 0$. Suppression of meridional flux and shift of flux to higher wavenumbers is seen in (*b*).

Very roughly (27) will agree with a simple mixing-length estimate. See also the derivation of Ho (1982). More careful calculation requires accurate evaluation of $\xi(k)$. One remark, however, is that $\xi(k)$ tends to be an increasing function of k and therefore dominant contributions to fluxes $\langle \boldsymbol{u}\phi \rangle$ will occur on lengthscales slightly larger than dominant energetic lengthscales. Figure 5(*a*) from a numerical simulation (64×64, pseudospectral, dealiased) shows this tendency.

Another special case is anisotropic turbulence without β. Then $R \neq 0$, D_{11} varies as $1 + R/2$. Recalling that $R > 0$ gives the tendency to prefer zonal (u_1) over meridional (u_2) motions, this is seen to be a natural result. Having assumed the low-order truncation (22), we are obliged to consider motion fields close to isotropy ($R^2 < 1$).

The effects of β may be the most interesting of all. In part β has a strong indirect effect due to the tendency to induce anisotropy in the velocity field favouring $R > 0$

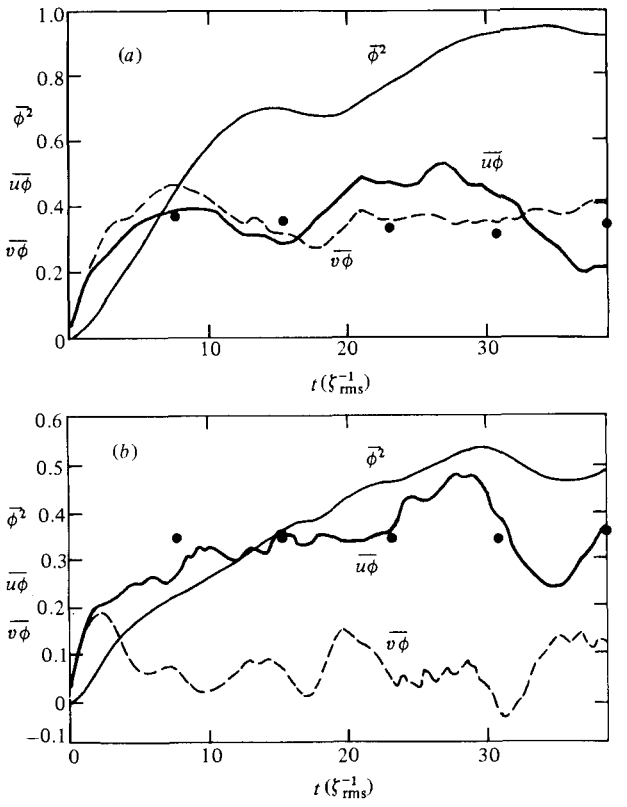

FIGURE 6. Time evolution of total tracer variance $\overline{\phi^2}$ and total fluxes $\overline{u\phi}$ and $\overline{v\phi}$, each quantity averaged over the flow domain, is shown for two cases: (*a*) $\beta = 0$; (*b*) $\beta \neq 0$. Dots show simple mixing-length estimates ($= 2\times$ kinetic energy/r.m.s. vorticity) for comparison.

(cf. Rhines 1975; Holloway & Hendershott 1977). However, apart from production of $R > 0$, β has direct effects due to finite δ in I_n. From figure 4 we see that increasing β, hence decreasing δ, reduces values of I_0 and I_2 while producing positive values in I_1. Ignoring R, we see from (24) that D_{11} varies as $I_0 + I_1$ while D_{22} varies as $I_0 - I_1$. The result is that D_{11} is little affected by β while D_{22} is more strongly suppressed.

Because δ decreases toward small k, contributions to $v\phi$ are suppressed in the longer scales, i.e. just the more rapidly propagating waves. Thus contributions to $v\phi$ are shifted to shorter scales, a tendency which competes with the shift to longer scales shown in figure 5 (where $\beta = 0$).

The role of β is seen also in figure 6. By means of isotropically distributed external torques, a statistically stationary, nearly isotropic eddy field has been obtained. At an instant defined to be $t = 0$, a uniform tracer gradient $\boldsymbol{G} = (1, 1)$ is imposed. In figure 6(*a*) a value $\beta = 0$ is maintained. Fluxes $\overline{u\phi}$ and $\overline{v\phi}$ arise and saturate after about $t = 2\pi\zeta_{\rm rms}^{-1}$ while tracer variance continues to accumulate. With $\beta \neq 0$ in figure 6(*b*), fluxes arise but $\overline{v\phi}$ quickly saturates at a small value while $u\phi$ grows toward a value only somewhat less than in the $\beta = 0$ case.

A normalized correlation coefficient

$$C = \frac{|\overline{u\phi} + \overline{v\phi}|}{(\overline{u^2} + \overline{v^2})^{\frac{1}{2}} (\overline{\phi^2})^{\frac{1}{2}}}$$

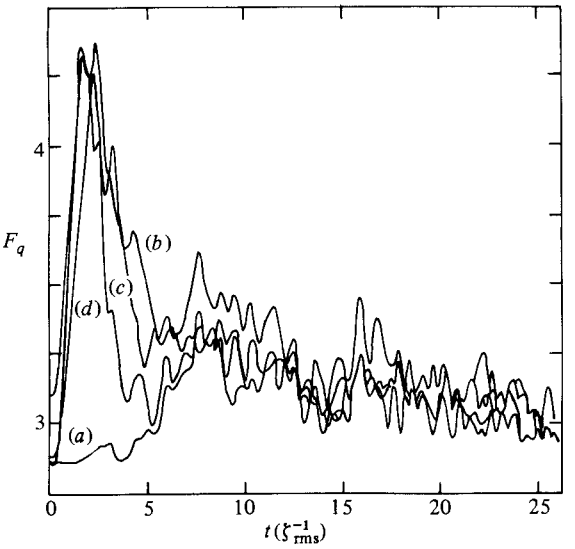

FIGURE 7. Intermittency as measured by flatness factors F_q is shown in an unforced, non-dissipative case. F_q are shown for four quantities: (*a*) $q = \phi$; (*b*) $q = \partial_x \phi$; (*c*) $q = \partial_y \phi$; (*d*) $q = \nabla^2 \phi$. As the fields evolve toward statistical equilibrium, flatness factors relax toward the Gaussian value $F_q = 3$.

in the isotropic ($\beta = 0$) case measures the efficiency of the gradient transport. At early times, C is large, with values 0.7–0.8. As ϕ-variance accumulates, the value of C decreases toward a saturation value near 0.3–0.4. When $\beta \neq 0$, the meridional flux may be quite small. Nonetheless a zonal correlation coefficient

$$\frac{|\overline{u\phi}|}{(\overline{u^2})^{\frac{1}{2}}(\overline{\phi^2})^{\frac{1}{2}}}$$

also saturates at a value near 0.3–0.4.

7. Intermittency

Second-moment (EDQNM) closure theory has a weakness. By describing only second-moment statistics, the theory fails to anticipate the extent to which fields may become patchy or intermittent. In fact EDQNM theory is consistent with intermittency inasmuch as one does not assume that higher cumulants vanish. Rather, EDQNM makes simplifying assumptions about relations among cumulants. The goal is to evaluate triple moments $\langle\zeta\zeta\zeta\rangle$, $\langle\zeta\zeta\phi\rangle$ and $\langle\zeta\phi\phi\rangle$ in (9). For truly random-phase, hence Gaussian, fields triple moments would vanish. Effectively EDQNM supposes that fourth and higher non-Gaussian moments arise in conjunction with non-vanishing triple moments.

A common measure of intermittency is kurtosis or flatness factor $F_q = \overline{q^4}/(\overline{q^2})^2$, where q denotes the field of interest. For Gaussianly distributed q, $F_q = 3$. An excess $F_q - 3 > 0$ indicates intermittency. In most cases we do not have quantitative forecasts for F_q. An exception occurs in cases of evolution toward unforced, undamped statistical equilibrium, as described in §3. Near equilibrium (8), fields approach their maximally random state, which would be seen in $F_q \to 3$. Other cases such as stirring in the presence of a mean gradient will sustain variance transfer (i.e. non-vanishing triple moments) and hence some sustained level of $F_q > 0$.

The approach to (8) is an instructive situation in which to examine intermittency. Based upon direct numerical simulation, figure 7 shows evolution of flatness factors.

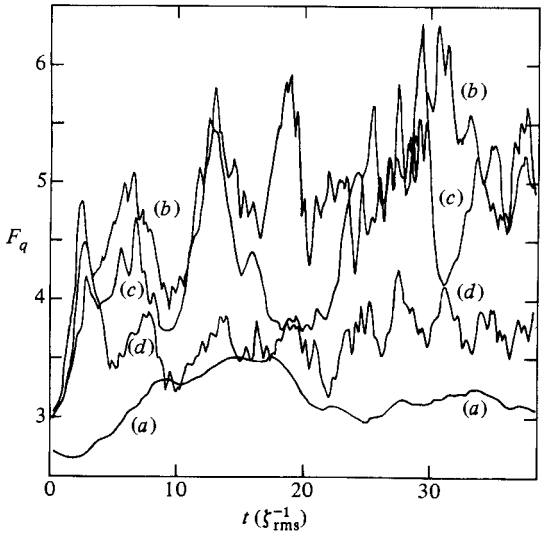

FIGURE 8. Intermittency as measured by flatness factor F_q is shown in the case where a mean gradient G as well as dissipation is present. Flatness factors, especially for the derivative fields ϕ_x and ϕ_y, approach quasistationary values above the Gaussian value 3. Curves are coded as in figure 7.

$\overline{q^4}/(\overline{q^2})^2$ where q represents ϕ, $\partial_x\phi$, $\partial_y\phi$ and $\nabla^2\phi$. The initial field consists of random phase assignments independently for ϕ and for ζ subject to a prescribed variance spectrum. Because of the random phase assignment, initial ϕ- and ζ-fields (and their derivatives) have nearly Gaussian probability distributions (by the central-limit theorem). At $t = 0$ flatness factors are close to the Gaussian value 3. After $t = 0$ variance transfer develops as the flow moves towards (8). Variance transfer requires non-Gaussian moments. In the later approach to (8), variance transfer relaxes toward zero and figure 7 shows flatnesses relaxing toward 3. The case of stirring in the presence of a mean gradient is seen in figure 8, which shows sustained levels of excess F_q especially in the derivative fields $\partial_x\phi$ and $\partial_y\phi$. Sustained levels of derivative kurtosis are symptomatic of such forced, dissipative, disequilibrium balances.

8. Stirring from an initial spot

For the most part, this paper is concerned with variance transfer and with the stirring down from large-scale mean fields. Physical intuition as well as many practical interests concern the complementary problem of stirring out from an isolated initial spot, e.g. as a dye-release experiment (Ewart & Bendiner 1981) or an accidental contaminant spill (Kupferman & Moore 1981).

No very adequate theory appears to exist for the initial-spot scenario. Even a choice of measures by which to describe spot evolution is ambiguous. In this section we resort to numerical simulation in order to provide an illustration of a spot evolution and to compare a variety of measures. See further the studies by Haidvogel & Keffer (1984).

For equations of motion we choose

$$\partial_t(\nabla^2-\alpha^2)\,\Psi+\beta\,\partial_x\,\Psi+\mathrm{J}(\Psi,\nabla^2\Psi)+\delta\nabla^6\Psi=0, \tag{28a}$$

$$\partial_t\phi+\mathrm{J}(\Psi,\phi)+\delta\nabla^4\phi=0. \tag{28b}$$

These are (1) expressed in terms of a stream function Ψ where $\zeta = \nabla^2\Psi$. Jacobian terms express the advective terms in (1). We include in (28*a*) a geophysically plausible inverse deformation radius α. *Ad hoc* choices for D_ζ and D_ϕ in (1) are

$$D_\zeta = D_\phi = -\delta\nabla^4. \tag{29}$$

Justification for (29) is only that it represents, albeit crudely, effects of unresolved, small-scale processes leading to variance dissipation, thus preventing unphysical evolution toward (8). We may interpret the role of (29) as setting an effective Batchelor scale L_B, where

$$L_B^4 = \delta/\epsilon^{\frac{1}{3}} \tag{30}$$

and ϵ is the average dissipation rate for vorticity variance. L_B is the lengthscale at which straining effects estimated by $\epsilon^{\frac{1}{3}}$ compete with the effect of (29), resulting in smoothing of small scales up to about $2\pi L_B$.

Physical scales for the simulation are as follows:

L = length of flow domain = 1000 km,
α^{-1} = inverse deformation radius = 50 km,
$\beta = 2.0 \times 10^{-11}$ m^{-1} s^{-1},
$u_{\text{rms}} = 7$ cm s^{-1},
$2\pi L_B = 20$ km,
T = duration of experiment = 4 months.

To achieve better representation over a broader range of scales, we have increased resolution to correspond to 128×128 grid points, hence to a grid spacing of $\Delta x = 8$ km.

A velocity field has been generated during a period of forcing by random torques. From the initiation of the spot experiment at nominal $t = 0$, all forcing of the velocity field is omitted. Thus the velocity field decays slowly so that, over the four-month experiment, kinetic energy decreases only slightly although vorticity variance decreases to 40 % of its initial value.

Dispersal of a spot is sometimes interpreted in terms of dispersal of a number of neutral particles. Such particles may be seeded as a part of a dye-release experiment. We initialize nine particles in the dye spot and follow their subsequent motion according to $\mathrm{d}\boldsymbol{x}/\mathrm{d}t = \boldsymbol{u}$.

Figure 9 shows evolution of the stream-function field at two-week intervals. A number of features should be noted. There is no marked anisotropy in the stream function despite significant β. Plausibly this is due to a moderating role of α. Secondly, there is visible growth of scale over the four month period, a characteristic of decaying two-dimensional turbulence. Thirdly, a tendency for westward propagation of pressure ridges and troughs is discernible. Fourthly, positions of the nine Lagrangian particles are marked in each frame. Especially the reader should note that the Lagrangian particles have become well dispersed over the flow domain. (Note that periodic boundary conditions apply also to particles. A particle exiting through an eastern boundary, say, re-enters from the west.)

Dispersal of the tracer field is shown in figure 10 at the instants for which the stream function is shown in figure 9. Contour intervals are fixed in linearly spaced increments of absolute concentration. As concentration fades by dilution, contour lines are lost. Initial concentration is a Gaussian spot located by chance on the western edge of a northward jet. During the first month, the northward jet propagates across the spot location, resulting in a northward displacement as well as the first of an apparent

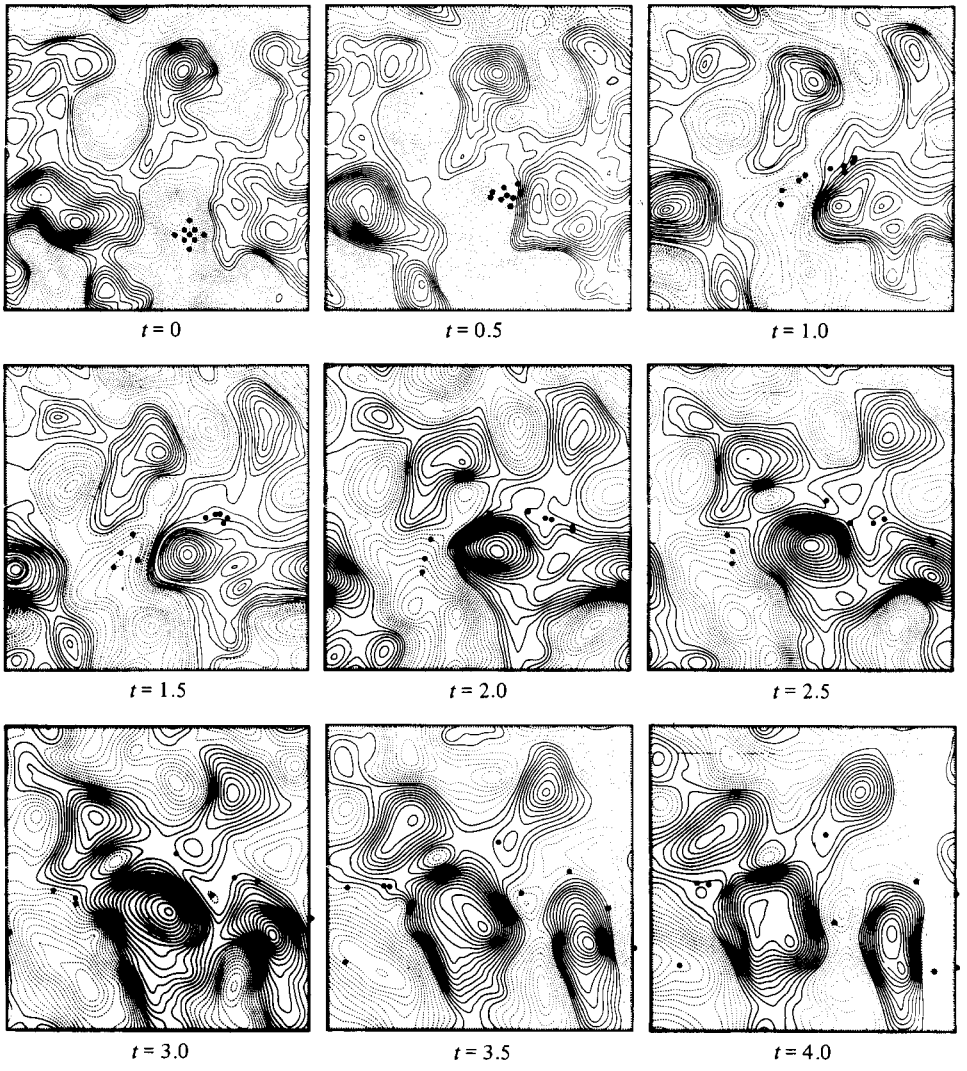

FIGURE 9. Evolution of stream function $\psi(\boldsymbol{x}, t)$ is shown at intervals of 0.5 months over a simulated four-month experiment. Positions of nine Lagrangian floats are marked.

'sequence of splittings'. Over the four-month period there is more zonal than meridional dispersal.

At $t = 4$ months some tracer has been dispersed throughout the flow domain, yet figure 10 shows little tendency to fill in the background field. However, since much of the tracer has diluted to levels below the lowest contour increment, it would seem possible that homogenization (filling in the background) is proceeding in the weak concentration field. To examine this possibility, figure 11 shows only tracer at weaker concentrations with contour increments at 0.1 of the increments in figure 10. A qualitative impression is that homogenization proceeds rather ineffectively despite the fact that tracer has been dispersed over scales larger than characteristic eddy fields, an observation bearing on discussions of 'streakiness' (Garrett 1981, 1983; Hollloway 1982; Keffer & Haidvogel 1982; Haidvogel & Keffer 1983). In particular, although the area of a 'domain of occupation' (Kupferman & Moore 1981) sufficient to enclose most of the tracer has increased roughly 100-fold by $t = 4$, peak concentra-

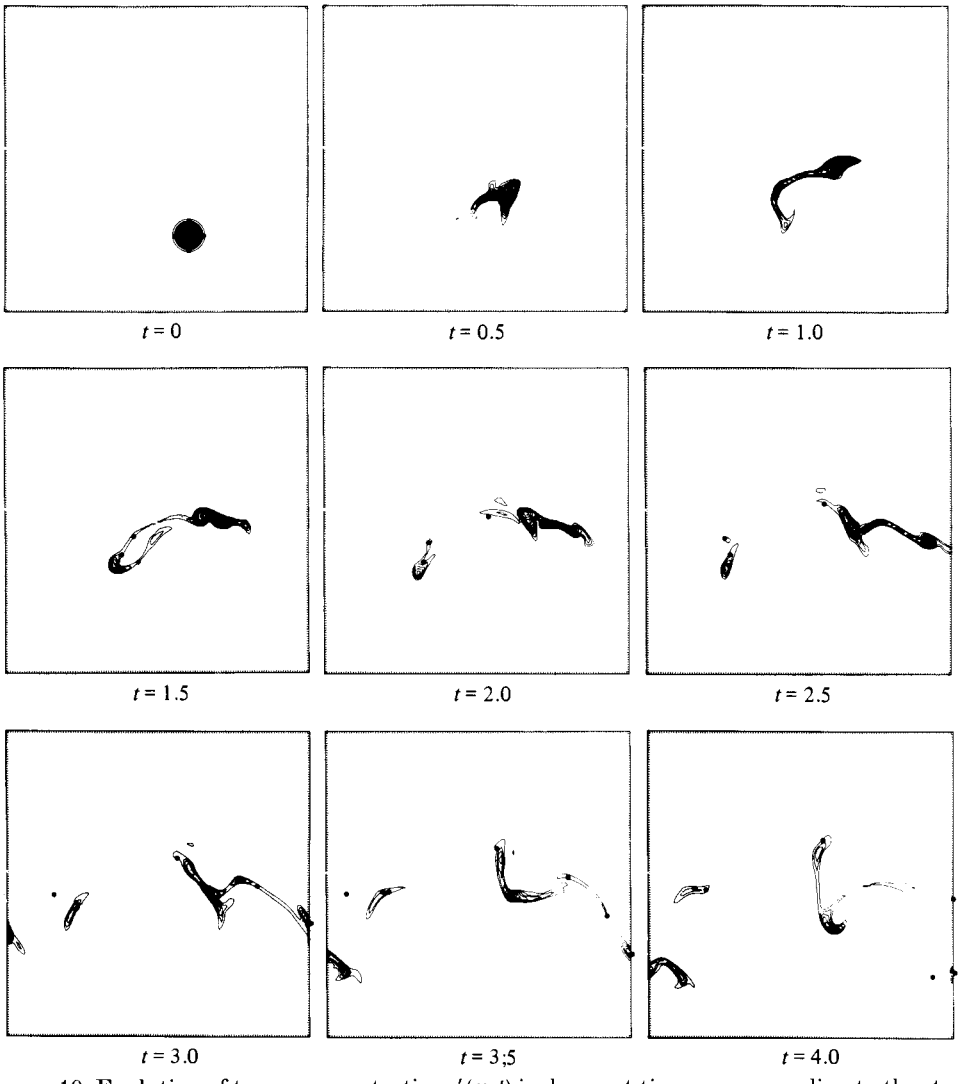

FIGURE 10. Evolution of tracer concentration $\phi(\boldsymbol{x}, t)$ is shown at times corresponding to the stream function seen in figure 9. Contour intervals are fixed, linearly spaced increments of absolute concentration.

tion has only been reduced to 0.24 of the peak concentration at $t = 0$. However, it should be noted that this result will have some sensitivity to choice of the D_ϕ operator in (1*b*). In particular, $\mathrm{D}_\phi = \nabla^4$ will not ensure a maximum principle, i.e. that extremal values be reduced in their ranges.

A variety of measures might be devised in order to characterize stirring from an initial spot. Choice of such a measure could be based, for example, on some aspect of environmental impact concern. Among the more familiar measures are the growth rates of centred second moments

$$\left.\begin{aligned} V_x &= \iint \mathrm{d}x\,\mathrm{d}y\,(x - x_{\mathrm{cm}})^2\,\phi, \\ V_y &= \iint \mathrm{d}x\,\mathrm{d}y\,(y - y_{\mathrm{cm}})^2\,\phi, \end{aligned}\right\} \tag{31}$$

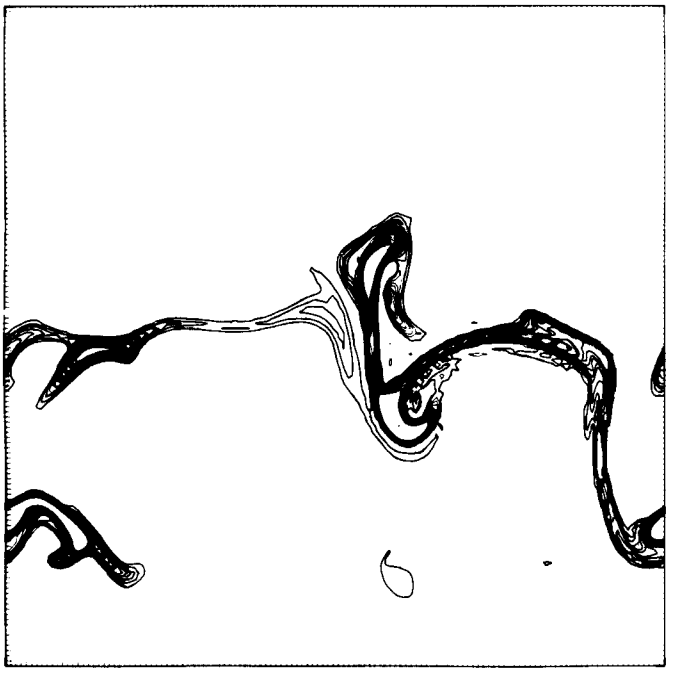

FIGURE 11. Tracer concentration at $t = 4$ months in figure 10 is recontoured. Contour increments are one tenth of those in figure 10. Only weaker levels of concentration are shown.

where (x_{cm}, y_{cm}) is the centroid of the ϕ-distribution. Measures based on Lagrangian particle statistics include single-particle dispersion

$$\left.\begin{aligned} S_x &= \overline{(X(t)-X(0))}^2, \\ S_y &= \overline{(Y(t)-Y(0))}^2, \end{aligned}\right\} \tag{32}$$

where overbars denote the average over all particles. Because (32) is based only upon a finite number of particles, and because the centroid motion is not removed in (32), these measures may evolve differently from (31). If eddy effects were to act analogously to diffusion, each of the moments (31) and (32) would grow proportionally to t. However, it is seen in figure 12 that zonal moments V_x and S_x grow as t^2. (After $t = 3$, dye re-enters and V_x is invalid. Absolute particle positions are retained, though plotted periodically; hence S_x remains valid.) Scaling of second moments as t^2 is known empirically as 'diffusion-velocity' scaling. Both V_y and S_y show much less effective meridional dispersal.

After $t = 1$, S_y shows essentially no growth. Prior to $t = 1$, rapid growth of S_y as t^2 is due to centroid dispersion, i.e. the centroid of particles is displaced northward. Effects of centroid dispersion may be removed by considering Lagrangian pair-separation statistics,

$$D_L = \overline{(X_i - X_j)}^2 + \overline{(Y_i - Y_j)}^2, \tag{33}$$

where overbars denote the average over each (i,j) particle pair. Evolution of D_L is also shown in figure 12, again approximating t^2 or 'diffusion-velocity' scaling. This result is empirical. The present experiment does not show the onset of eddy-diffusion scaling, i.e. second-moment growth proportional to t.

There is a caution which is especially to be noted in this section. The result of one

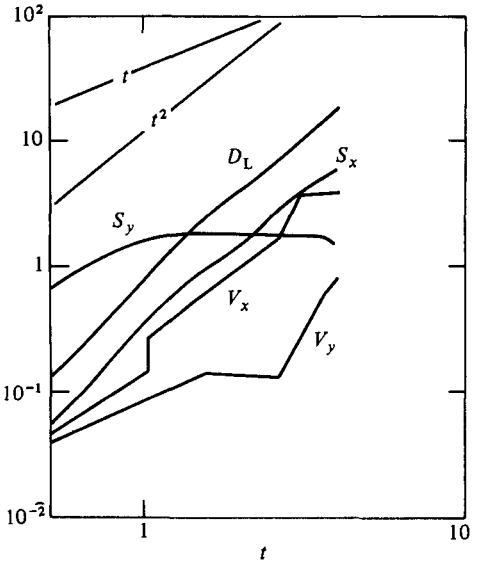

FIGURE 12. Eulerian and Lagrangian measures of spot growth as defined in (31)–(33) are shown for the experiment seen in figures 9 and 10. Added lines show growth laws as t and t^2 for comparison.

or even several (Haidvogel & Keffer 1984) spot-release experiments may not be statistically reliable. However, this aspect threatens the interpretation from actual deliberate-release experiments (Ewart & Bendiner 1981) and casts doubt on the predictability of dispersal from an accidental release (Kupferman & Moore 1981). The difficulty is that we are seeking to describe dispersal on the same scales as the dispersing agents, the eddies. Individual realizations depart widely from ensemble expectations.

This situation is different from the gradient-transport phenomena considered in §6. There, the transport results from many, relatively independent, eddy-stirring events, contributing to the statistical reliability of a single flow-field realization. Moreover, for the uniform-gradient case, the lengthscale of variation of mean field is infinitely large compared with eddy scales. For these reasons we argue that the concept of eddy diffusivity is appropriate to cases of smaller-scale eddies stirring substance down (and across) large-scale property gradients, but that eddy diffusivity is an inappropriate or misleading concept as applied to initial-spot dispersal.

9. Summary and outlook

Among the many processes that lead to stirring and transport in geophysical flows, we have focused upon the larger-scale, nearly horizontal or parapycnal stirring. We have further idealized the flow as two-dimensional geostrophic motion on a beta-plane. These are severe idealizations. Nonetheless, a wealth of complicated phenomena remain. We feel that a quantitative as well as qualitative understanding at this level will be requisite to an understanding at any more advanced level of dynamics.

For the problem that we have defined, we have tried to adopt an encompassing approach. We have considered the problem by methods of direct numerical simulation, turbulence-closure theory and equilibrium statistical mechanics.

Broadly, phenomena examined here fall into three groups. In the first group, we consider statistically homogeneous fluctuation fields with no mean fields present. The

main emphasis is upon transfer of variance across a wavenumber spectrum. Closure theory predicts, and numerical experiments confirm, that variance of the passive tracer is transferred more rapidly than vorticity variance despite the fact that both passive tracer and vorticity are advected quantities. The reason for this difference is that wavenumber–local interactions can be quite effective at transferring passive tracer variance, whereas, in two-dimensional flow, local interactions cannot transfer vorticity variance. A result is that total variance of passive tracer decays more quickly than total vorticity variance. We note that the equilibrium statistical-mechanical solutions also differ for passive tracer and for vorticity. Although our methods and results are given in Eulerian field variables, we suggest that the Lagrangian autocorrelation for passive tracer decays more quickly than the vorticity autocorrelation; this is seen in numerical experiments.

In a second area of study, we have treated statistically homogeneous fluctuations in the presence of a uniform gradient of passive tracer concentration. Presence of the gradient term induces cross-correlation between the tracer and the velocity fluctuations. Closure theory and numerical experiments yield consistent results. For horizontally isotropic turbulence with $\beta = 0$, a net down-gradient tracer transport occurs. Magnitude of an effective diffusivity agrees approximately with simple mixing-length estimates. Examination of the tracer–velocity cross-spectrum shows that most of the spatial transport is born by scales somewhat larger than the scales of most energetic eddies. When $\beta \neq 0$, meridional transport is strongly suppressed relative to zonal transport. Thus non-zero β induces anisotropy in the eddy-diffusivity tensor.

Thirdly, we contrast the stirring down on a uniform gradient with a numerical simulation of stirring out from an initial tracer spot. We compare various statistics of the tracer evolution with statistics of a number of Lagrangian particles also released in the initial spot. Although growth of second spatial moments, either of tracer field or of Lagrangian particle ensemble, could be fitted to a scale-dependent diffusivity, such a description may be misleading. We observe tracer dispersed over distances substantially larger than the largest eddy lengthscales; yet the tracer field remains quite streaky, i.e. consisting of relatively undiluted filaments. We further remark that initial-spot experiments are expected to be highly variable from one release to another. Initial-spot experiments are therefore difficult to characterize or to anticipate.

We consider intermittency as measured by the departure of fluctuation statistics from Gaussian distribution. We demonstrate that, for unforced non-dissipative flow, intermittency vanishes as the flow relaxes toward the statistical-mechanical equilibrium. Contrariwise, we observe that, for dissipative flow in the presence of a mean gradient, non-Gaussian moments arise and achieve stationary values.

The present study could be extended in many ways. For example, closure theory as developed in §4 has not been tested and calibrated quantitatively in a study such as Herring *et al.* (1982). The role of finite deformation radius has been included in §8, but not in the previous sections. It would be useful to extend this study throughout to include cases where the energetic eddy lengthscale is as large as, or larger than, the effective deformation radius. (Motions on scales larger than the deformation radius would be particularly appropriate to plasma-transport problems mentioned in §1, for which the quantity analogous to deformation radius is the ion gyroradius.)

Another topic of current interest is the possible role of isolated long-lived vortices in the stirring and transport of substance. Methods of statistical mechanics or

turbulence-closure theory as given in this paper are not directly applicable. A numerical simulation study of passive tracer stirred and transported in the evolving velocity fields of isolated vortices is reported in Riser & Holloway (1984).

Extension of present work to include mean-flow fields, especially closed gyre circulations, is an important objective. As a first step, present results may be used to specify spatially variable, anisotropic diffusivities within larger circulation patterns (cf. Armi & Haidvogel 1982). However, the validity of the eddy-diffusivity form depends upon scale separation between eddies and the variation of mean properties, including mean flow. Sufficient scale separation may not be realized in actuality. Theoretical approaches may develop along lines of quasi-homogeneity, as in Carnevale & Martin (1982) or Ho (1982).

Other extensions could include baroclinically active flow (raising interesting questions about the relationship between horizontal tracer transport and the rate of release of available potential energy) and flow overlying irregular topography. Theoretical approaches to stirring in such complicated situations may prove impractical. However, numerical simulation should remain as a straightforward, viable approach.

This work has been supported in part by the National Science Foundation under grant OCE-7923546. Computations have been performed at the National Center for Atmospheric Research, which is sponsored by the National Science Foundation. We are grateful for comments from Dr C. J. R. Garrett and from anonymous referees. Programs for the direct simulations have evolved as a group effort including contributions from Dr M. K. Davey, Dr D. B. Haidvogel and Dr S. Riser. This is contribution number 1365 of the School of Oceanography of the University of Washington.

REFERENCES

Armi, L. & Haidvogel, D. B. 1982 Effects of variable and anisotropic diffusivities in a steady-state diffusion model. *J. Phys. Oceanogr.* **12**, 787–794.

Basdevant, C., Legras, B., Sadourny, R. & Béland, M. 1981 A study of barotropic model flows: intermittency, waves and predictability. *J. Atmos. Sci.* **38**, 2305–2326.

Bennett, A. F. & Haidvogel, D. B. 1983 Low-resolution numerical simulation of decaying two-dimensional turbulence. *J. Atmos. Sci.* **40**, 738–748.

Carnevale, G. F., Frisch, U. & Salmon, R. 1981 *H*-theorems in statistical fluid dynamics. *J. Phys.* A: **14**, 1701–1718.

Carnevale, G. F. & Martin, P. C. 1982 Field theoretical techniques in statistical fluid dynamics: with application to nonlinear wave dynamics. *Geophys. Astrophys. Fluid Dyn.* **20**, 131–164.

Chatwin, P. C. & Sullivan, P. J. 1980 Some turbulent diffusion invariants. *J. Fluid Mech.* **97**, 405–416.

Davis, R. E. 1983 Oceanic property transport, Lagrangian particle statistics, and their prediction. *J. Mar. Res.* **41**, 163–194.

Deem, G. S. & Zabusky, N. J. 1971 Ergodic boundary in numerical simulation of two-dimensional turbulence. *Phys. Rev. Lett.* **27**, 396–399.

Durbin, P. A. 1980 A stochastic model of two-particle dispersion and concentration fluctuations in homogeneous turbulence. *J. Fluid Mech.* **100**, 279–302.

Ewart, T. E. & Bendiner, W. P. 1981 An observation of the horizontal and vertical diffusion of a passive tracer in the deep ocean. *J. Geophys. Res.* **86**, 10974–10982.

Fox, D. G. & Orszag, S. A. 1973 Inviscid dynamics of two-dimensional turbulence. *Phys. Fluids* **16**, 169–171.

FREDERIKSEN, J. S. & SAWFORD, B. L. 1980 Statistical dynamics of two-dimensional inviscid flow on a sphere. *J. Atmos. Sci.* **37**, 717–732.

FRISCH, U., LESIEUR, M. & BRISSAUD, A. 1974 A Markovian random coupling model for turbulence. *J. Fluid Mech.* **65**, 145–152.

GARRETT, C. J. R. 1981 Streakiness. *Ocean Modelling* 41 (unpublished manuscript).

GARRETT, C. J. R. 1983 On the initial streakiness of a dispersing tracer in two- and three-dimensional turbulence. *Dyn. Atmos. Oceans* (submitted).

HAIDVOGEL, D. B. 1982 On particle tracking in Eulerian ocean models. *Ocean Modelling* 45 (unpublished manuscript).

HAIDVOGEL, D. B. & KEFFER, T. 1984 Tracer dispersal by mid-ocean mesoscale eddies. I: Ensemble statistics. *Dyn. Atmos. Oceans* (submitted).

HASEGAWA, A., MACLENNAN, C. G. & KODAMA, Y. 1979 Nonlinear behavior and turbulence spectra of drift waves and Rossby waves. *Phys. Fluids* **22**, 2122–2129.

HERRING, J. R., SCHERTZER, D., LESIEUR, M., NEWMAN, G. R., CHOLLET, J. P. & LARCHEVEQUE, M. 1982 A comparative assessment of spectral closures as applied to passive scalar diffusion. *J. Fluid Mech.* **124**, 411–437.

HILL, J. C. 1981 Heat transfer in isotropic turbulence. *Chem. Engng Commun.* **12**, 69–96.

HO, L. 1982 Weakly inhomogeneous turbulence with applications to geophysical flows. Ph.D. thesis, MIT and NCAR.

HOLLOWAY, G. 1976 Statistical hydromechanics: application in mesoscale ocean circulation. Ph.D. thesis, Univ. Calif. San Diego.

HOLLOWAY, G. 1982 A comment on streakiness. *Ocean Modelling* 43 (unpublished manuscript).

HOLLOWAY, G. & HENDERSHOTT, M. C. 1977 Stochastic closure for nonlinear Rossby waves. *J. Fluid Mech.* **82**, 747–765.

KEFFER, T. & HAIDVOGEL, D. B. 1982 Numerical simulations of tracer streakiness. *Ocean Modelling* 45 (unpublished manuscript).

KRAICHNAN, R. H. 1967 Inertial ranges in two dimensional turbulence. *Phys. Fluids* **10**, 1417–1423.

KUPFERMAN, S. & MOORE, D. E. 1981 Physical oceanographic characteristics influencing the dispersion of dissolved tracers released at the sea floor in selected deep ocean study areas. *Sandia Natl Labs Rep.* SAND80-2573.

LESIEUR, M., SOMMERIA, J. & HOLLOWAY, G. 1981 Zones inertielles du spectre d'un contaminant passif en turbulence bidimensionelle. *C.R. Acad. Sci. Paris* **A II–20**.

LESLIE, D. C. 1973 *Developments in the Theory of Turbulence.* Clarendon.

ORSZAG, S. A. 1977 Statistical theory of turbulence. In *Fluid Dynamics, 1973 Les Houches Summer School of Theoretical Physics* (ed. R. Balian & J. L. Peube), pp. 235–374. Gordon & Breach.

RHINES, P. B. 1975 Waves and turbulence on a beta-plane. *J. Fluid Mech.* **69**, 417–443.

RHINES, P. B. 1977 The dynamics of unsteady currents. In *The Sea*, vol. 6, pp. 189–318. Interscience.

RISER, S. C. & HOLLOWAY, G. 1984 Horizontal mixing by isolated vortices. *Dyn. Atmos. Oceans* (submitted).

ROSE, H. A. & SULEM, P. L. 1978 Fully developed turbulence and statistical mechanics. *J. Phys. (Paris)* **39**, 441–484.

SALMON, R., HOLLOWAY, G. & HENDERSHOTT, M. C. 1976 The equilibrium statistical mechanics of simple quasi-geostrophic models. *J. Fluid Mech.* **75**, 691–703.

SHANNON, C. E. 1948 The mathematical theory of communication. *Bell Syst. Tech. J.* **27**, 379–423, 623–656.

SVERDRUP, H. V., JOHNSON, M. W. & FLEMING, R. H. 1942 *The Oceans: Their Physics, Chemistry and General Biology.* Prentice-Hall.

TAYLOR, G. I. 1921 Diffusion by continuous movements. *Proc. Lond. Math. Soc.* **20**, 196–212.

THIEBAUX, M. L. 1975 The linear mean gradient model for two-particle turbulent diffusion. *J. Atmos. Sci.* **32**, 92–101.

WALTZ, R. E. 1983 Numerical study of drift wave turbulence with simple models for wave–wave nonlinear coupling. *Phys. Fluids* **26**, 169–179.